9-1980

Continuous Digital Simulation of the Second-Order Slowly Varying Wave Drift Force

Bohdan W. Oppenheim
Loyola Marymount University, boppenheim@lmu.edu

P. A. Wilson

Recommended Citation

Oppenheim, B.W. and Wilson, P.A. (1980) Continuous digital simulation of the second-order slowly varying wave drift force. Journal of Ship Research, 24, (3), 181-189.

Journal of Ship Research, Vol. 24, No. 3, Sept. 1980, pp. 181–189

Continuous Digital Simulation of the Second-Order Slowly Varying Wave Drift Force

B. W. Oppenheim[1] and P. A. Wilson[1]

A discussion is given on practical aspects of digital representation in time of the slowly oscillatory second-order wave drift force from a known force spectrum. The emphasis is placed on the computational efficiency and on the suitability of the simulation to a numerical integration of an equation of motion using a variable integration step size, where the force acts as the excitation of motion. The effect of approximating the original spectrum by a white spectrum is discussed. A sensitivity analysis is made to the range of frequencies of the spectra. The force time record is obtained by first generating at equal time intervals a discrete time series which possesses the desired random characteristics, and then by extending the discrete series into a continuously available digital record using a $\sin(x)/x$-type interpolation. Various numerical tests are illustrated with plots. Superiority of the fast Fourier transform over the cosine series is demonstrated in terms of the spectral contents preservation.

Introduction

THE HYDRODYNAMIC force acting upon a vessel floating in waves contains a first-order component with zero mean and proportional to the wave amplitude, and a second-order component proportional to the square of the wave amplitude. The first-order force contains harmonics of frequencies equal to the wave harmonics only. The second-order component, commonly called drift force, is constant in regular waves and if the waves are irregular it also contains oscillatory parts. The latter are associated with occurrence of wave groups, and are of frequencies much lower than the wave frequencies. The drift force in spite of its second-order magnitude can cause large motions of the vessel if the corresponding static restoring force is low. Such a case occurs, for example, when a vessel is moored. The resonance of horizontal motions of a moored vessel occurs at frequencies with high power content of the drift force spectrum, thus resulting in relatively large motions.

The equations of motion which describe the horizontal motions of moored floating vessels are nonlinear, coupled, and contain feedback. The nonlinearities are due to the nonlinear characteristics of the mooring restoring force (catenary effects) and nonlinear (approximately cubic) dependence of the damping force with the vessel velocity. The coupling exists in general between the sideways (sway) and rotational (yaw) modes of motion due to hydrodynamic and inertial asymmetry of the forward and aft portions of the vessel; it is due as well to the directional coupling of mooring restoring force. The feedback occurs due to the dependence of the drift force on the relative heading of the waves (that is, on the yaw motion indirectly). Because of the nonlinearities, the simulated response of the vessel may be ill-behaved; that is, it may demonstrate rapid variations of direction and magnitude. Also, the numerical integration itself may introduce a progressively increasing numerical error which may eventually lead to the numerical instability of the solution. The only remedy available for overcoming the numerical instabilities and, simultaneously, for accurate detection of rapid variations of the response, is to decrease the time step size of the integration to an acceptably small value usually determined only by experimentation. A small step may result in lengthy computations. For example, if a statistical analysis is to be made of the motion, the record duration should correspond to several hundred "typical" cycles. Frequently, in order to detect the rapid changes of the response, it is necessary to use a step size on the order of one-hundredth of the cycle period. Thus the total number of steps in the integration may easily reach tens of thousands. Consequently, it is desirable from the point of view of computational efficiency to introduce a variable step size. During an ill-behaved response the step is kept small to detect all rapid variations, and it is increased during "regular" portions of the responses to increase the speed of the integration.

The method of digital integration using a variable step size requires special techniques of simulating the excitation in the equation of motion, if the excitation is to represent a random signal. The need for special techniques arises because the time of the next integration point is not known a priori; consequently the excitation signal value may be required at any point in time and it must therefore be available continuously, although by a discrete digital value. Two such techniques are discussed in this paper.

The drift force spectrum has a very particular shape which yields itself to an approximation by a band-limited white spectrum. The quality of the approximation depends on the frequency bandwidth, and these problems are also discussed here. The last topic covered is the rationale for selecting the cutoff frequency of the spectrum, the sensitivity of the signal quality to this selection, and the constraints imposed on the selection by the physics of the problem.

The discussion is limited to a single degree of freedom. This removes the need to consider resolving the drift force in terms of spatial components, cross-coupling, and the associated feedback phenomenon.

'Exact' drift force spectrum and its range of frequencies

It was shown in [1][2] that the mean drift force, F, and its slowly oscillatory spectrum, S_F, have the form

$$F = C_1 \int_0^\infty H_F(\omega) G_w(\omega) d\omega \qquad (1)$$

[1] Department of Ship Science, University of Southampton, Southampton, England. (Coauthor Oppenheim is on leave of absence from Global Marine Inc.)

Manuscript received at SNAME headquarters March 13, 1979; revised manuscript received January 25, 1980.

[2] Numbers in brackets designate References at end of paper.

$$G_F(\mu) = C_2 \int_0^\infty H_F^2\left(\omega + \frac{\mu}{2}\right) G_w(\omega) G_w(\omega + \mu) d\omega, \qquad \mu > 0, \text{ small} \quad (2)$$

where $H_F(\omega)$ is the second-order drift force transfer function and $G_w(\omega)$ is the wave amplitude spectrum (one-sided). C_1 and C_2 are two constants. The random force and the resulting vessel motions are assumed stationary. Consequently, it is a simple matter to remove the dc signal from both the excitation and the response. Thus the following discussion can be limited to the oscillatory portions of the signals only.

The typical shape of $G_F(\mu)$ is shown in the upper frame of Fig. 13 by a heavy line. The range of frequencies of $G_F(\mu)$ is large, but equation (2) has been derived with the assumption that μ is small. The immediate question is therefore where the cutoff frequency should be taken. The requirement of small μ implies that the force signal should be narrow-band and regular. The other requirement for a small cutoff frequency is the characteristics of the numerical integration procedure. If the excitation signal is narrow-band, the integration step size can be relatively large. In order to detect the response subjected to a wide-band excitation, the step would have to be small and even that may not prevent a numerical instability of the integration from occurring. On the other hand, in order to analyze the response statistically and in particular to obtain the least-square response transfer function for as wide a frequency range as possible, the cutoff frequency of the excitation spectrum should be as large as possible. The cutoff frequency should be significantly larger than the moored vessel resonant frequencies.

Nonlinear systems may also respond in the bifurcation mode and, to detect this, the excitation frequency must be at least three times as large as the natural frequencies. Certainly, the cutoff frequency should be significantly larger than the moored vessel resonant frequencies.

Since equation (2) is a second-order convolution, the force spectrum shape is similar in all practical sea and vessel combinations. Of particular interest is the part of the spectrum at low frequencies where the spectrum is almost uniform. In this region, the spectrum can be approximated by a band-limited white spectrum. Equation (2) becomes

$$G_F(\mu) = C_2 \int_0^\infty H_F^2(\omega) G_w^2 d\omega = G_F^0 = \text{const} \quad (3)$$

Such an approximation permits a significant simplification of the force spectrum calculation and of the record simulation. The latter can be computed once, stored, and utilized for any application by only scaling it for different desired white spectra.

The sensitivity of the record to the frequency range as well as to the spectrum type is tested numerically later in the section on testing.

Continuous availability of the discrete spectrum

The numerical integration algorithm which uses a variable step size may require the excitation signal value at any arbitrary time. The signal must therefore be available as a continuous function of time, although in a discrete digital manner. A random signal that is generated from a certain distribution has its minimum and maximum and it can take any value in between every time it is "randomly" generated. Consequently, the time interval of the random signal generation becomes in effect the half-period of the highest harmonic present in the signal. If the interval is very small, as is the case with the variable step size integration, the relative contribution to the signal of such high-frequency components becomes totally inadmissible, both because it unreasonably raises the high-frequency portion of the spectrum and because it makes the numerical integration very slow and possibly unstable. The solution to this problem is to generate the signal in a semirandom, semideterministic way; namely, the signal should be generated at sufficiently large but equal time intervals as a random signal, from the desired distribution, and the intermediate values of the signal should be obtained by a suitable smooth interpolation. This way the spectral contents of the signal can be preserved and the signal can be available at any arbitrary time, as demanded by the integration algorithm.

Two methods of generating the desired random signal at equal intervals are discussed here. The first is based on the Inverse Discrete Fast Fourier Transform (IDFFT) and the second is to express the signal as a weighted cosine series (CS). The superiority of the former over the latter, in terms of computing time, has been well recognized for some time [2, 3]. The present paper demonstrates another aspect of the superiority of the FFT, namely, the preservation of the spectral contents. The two methods are discussed separately.

IDFFT method

The discrete estimate of a continuous, smoothed, two-sided spectrum is given as

$$S_F(\omega_k) \simeq \frac{N\Delta}{2\pi} X_k^* X_k \quad (4)$$

$$\omega_k = \frac{2\pi k}{\Delta N}, \; k = 0, \pm 1, \pm 2, \ldots, \pm \frac{N}{2} \quad (5)$$

where Δ is the time interval at which the signal is generated and X_k is defined by the Discrete Fourier Transform (DFT) of a time sequence $\{x_r\}$, r = 0,1, . . . ,N − 1 as follows

$$X_k = \frac{1}{N} \sum_{r=0}^{N-1} x_r e^{-i(2\pi kr/N)} \quad (6)$$

The time sequence $\{x_r\}$ is, from IDFFT

Nomenclature

$C_{1,2}$ = constants
f = frequency, Hz
F = mean force
$G_w(\omega)$ = wave spectrum, one-sided
$G_F(\omega)$ = force spectrum, one-sided
G_F^0 = white spectrum
$H(f)$ = transfer function
$H_F(\omega)$ = drift-force transfer function
$i(t)$ = signal of Dirac functions
$I(g)$ = Fourier transform of $i(t)$
$IDFFT$ = inverse discrete fast Fourier transform
j = subscript
k = subscript
K = number of terms in cosine series
M = magnitude parameter in the frequency perturbation
n = subscript
N = number of terms in IDFFT
r = subscript
$S(\omega)$ = one-sided force spectrum
t_j, t_i = discrete time
t = continuous time
u = dummy variable in integration
x = dummy variable
x_r, x_j, x_i = discrete signal in time
$x(t)$ = continuous signal in time
X_K = Fourier transform of x_r
X_i = Fourier transform of x_i
$X(f)$ = Fourier transform of $x(t)$
$\delta(t)$ = Dirac function in time
$\delta(g)$ = Dirac function in frequency
$\delta\omega$ = frequency perturbation
$\Delta\omega$ = frequency interval
Δ = time interval
$\chi^2 = Ki$ − square distribution
μ = frequency
ϕ_k, ϕ_i = random phase
ω_{i_0} = discrete frequency in cosine series
ω_i = perturbed discrete frequency in cosine series
ω_k = discrete frequency in Fourier transform

$$x_r = \sum_{k=0}^{N-1} X_k e^{i2\pi kr/N}, \quad r = 0,1,\ldots,N-1 \tag{7}$$

The DFT sequence is then, from equation (4)

$$|X_k| = \left[\frac{2\pi}{N\Delta} S_F(\omega_k)\right]^{1/2} \tag{8}$$

In the present problem $S_F(\omega)$ is available from the drift force spectrum. On the other hand, the phase is not available. In order that $\{x_r\}$ be Gaussian, the phase contained in X_k must be random and uniformly distributed between 0 and 2π. Denoting the phase angle by ϕ_k, the DFT sequence $\{X_k\}$ becomes

$$X_k = |X_k| e^{i\phi_k} = \left[\frac{2\pi}{N\Delta} S_F(\omega_k)\right]^{1/2} e^{i\phi_k} \tag{9}$$

Finally, substituting equation (9) into equation (7) and converting $S_F(\omega_k)$ to the one-sided spectrum of the drift force, $G_F(\omega_k)$, yields the required time series $\{x_r\}$

$$x_r = \sum_{k=0}^{N-1} \left[\frac{2\pi}{N\Delta}\frac{1}{2} G_F(\omega_k)\right]^{1/2} e^{i\phi_k} e^{i2\pi kr/N}, \quad r = 0,\ldots,N-1 \tag{10}$$

The N random values x_r are spaced on the time axis Δ apart. The interval Δ should not be confused with the sampling interval of the response signal. In general the two will be different.

The calculation of equation (9) is carried out in the numerical examples given here using the FFT algorithm. The details of it can also be found in reference [4]. The numerical examples given later in the section on testing illustrate the sensitivity of $\{x_r\}$ to the duration of Δ and to the length of the series, N, in equation (10). It seems worthwhile to mention here a few practical aspects of using the IDFFT algorithm for the present purpose. It is important to order the sequence $\{X_k\}$ as follows: $X_0 = 0$ since the process has zero mean:

$$X_j = X_k^*, k = 1,2,\ldots,\frac{N}{2}, j = N-1, N-2,\ldots,\frac{N}{2}+1$$

where the asterisk denotes the complex conjugate. Finally, the spacing between the spectral ordinates read from the given spectrum G_F must be equal to $2\pi/(N\Delta)$, so that only $N/2$ spectral ordinates are read from the one-sided spectrum G_F.

Weighted cosine series method

Shinozuka in [5] successfully demonstrates that the time record can be generated as follows:

$$x_j = x(t_j) = \sqrt{2}\sum_{i=0}^{K} [G_F(\omega_i)\Delta\omega]^{1/2} \cos(\omega_i^0 t_j + \phi_i), \quad j = 0,\ldots N \tag{11}$$

where

$G_F(\omega_i)$ = drift force spectrum discretized at N frequencies
$\Delta\omega = (\omega_{max} - \omega_{min})/K$
ϕ_i = random phase uniformly distributed between 0 and 2π
$\omega_i^0 = \omega_i + \delta\omega(t)$
$\omega_i = \omega_{min} + (i-1)\Delta\omega$
$\delta\omega$ = random perturbation of frequency, introduced in order to prevent the signal periodicity within the record, and uniformly distributed as follows

$$-\frac{\Delta\omega}{M} \leq \delta\omega \leq \frac{\Delta\omega}{M}$$

where M is typically equal to 20 to 40.

The statistics of equation (11) can be found in [5]. The record $\{x_j\}$ is generated at equal time intervals $\Delta = t_j - t_{j-1}$. Note that this method is more direct than that of the IDFFT, but it is not obvious which is more efficient computationally. A comparison of the computer overhead for the two methods is provided, together with a discussion of sensitivity of $\{x_j\}$ to the number of harmonics used in equation (11), and to the interval length, Δ. Again, this interval should not be confused with the sampling interval of the record signal. The only requirement imposed on Δ by equation (11) is that it is small enough for the largest ω_i to be reflected in the signal, that is, $\omega_{max} \leq \pi/\Delta$. In particular, Δ is independent of the number of harmonics, K. In contrast, the interval length and the number of harmonics N in equation (10) are closely related to each other.

Interpolation of the discrete signal

The discrete signal obtained by either of the two methods described in the previous sections is available at time intervals Δ. This signal may be regarded as the result of multiplying a continuous signal (unknown) by a signal $i(t)$ which consists of Dirac delta functions

$$i(t) = \sum_{n=-\infty}^{\infty} \delta(t-n) \tag{12}$$

This gives the discrete signal $x_i(t)$ where

$$x_i(t) = x(t) \cdot i(t) \tag{13}$$

and it is desired to determine $x(t)$. The multiplication in time, equation (13), corresponds to convolution in frequency

$$X_i(f) = \int_{-\infty}^{\infty} X(f-g)I(g)dg \tag{14}$$

where X_i, X, and I are Fourier transforms of x_i, x, and i, respectively. The transform of $i(t)$ is

$$I(g) = \frac{1}{\Delta}\sum_{n=-\infty}^{\infty} \delta\left(g - \frac{n}{\Delta}\right) \tag{15}$$

Equation (14) now becomes, from property of the Dirac function:

$$X_i(f) = \int_{-\infty}^{\infty} X(f-g)\frac{1}{\Delta}\sum_{n=-\infty}^{\infty}\delta\left(g-\frac{n}{\Delta}\right)dg = \frac{1}{\Delta}\sum_{n=-\infty}^{\infty} X\left(f-\frac{n}{\Delta}\right) \tag{16}$$

This indicates that the signal $x_i(t)$ has a transform with period $1/\Delta$. If $X(f)$ is zero when $|f| \geq 1/2\Delta$, that is, outside of the Nyquist frequency, then $X_i(f)$ is simply a periodic version of $X(f)$. Thus it is possible to determine $X(f)$ from $X_i(f)$ by multiplying $X_i(f)$ by Δ, or formally by $H(f)$, where

$$H(f) = \begin{cases} \Delta, & |f| \leq \dfrac{1}{2\Delta} \\ 0, & \text{otherwise} \end{cases} \tag{17}$$

That is

$$X(f) = X_i(f) \cdot H(f) \tag{18}$$

The multiplication in the frequency domain corresponds to a convolution in time. The inverse Fourier transform of $H(f)$ is

$$H(f)|_{-F} = \frac{\sin(\pi t/\Delta)}{(\pi t/\Delta)} \tag{19}$$

It follows that

$$x(t) = \int_{-\infty}^{\infty} \frac{\sin(\pi u/\Delta)}{(\pi u/\Delta)} x_i(t-u)du \tag{20}$$

Table 1 Parameters of output spectrum calculations from interpolated record

Record length, s (approximately)	15000
Sampling interval, s	15
Number of points in sample	1000
Number of trailing zeros	24
FFT series length	1024
Power of 2 in FFT algorithm	10
Smoothing interval, No. of points	11
Frequency resolution (bandwidth), Hz	0.000716
Nyquist frequency, Hz	1/30
χ^2 number	21
σ/m of spectral ordinates	0.3
Window type applied to record	cosine

The derivation of equations (12) through (20) followed that given by Jenkins and Watts in [6].

The discrete form of equation (20), used in digital computation, is

$$x(t) = \sum_{i=-K}^{K} \frac{\sin \frac{\pi}{\Delta}(t - t_i)}{\frac{\pi}{\Delta}(t - t_i)} x_i(t_i) \qquad (21)$$

The convergence of $x(t)$ with K is theoretically perfect; when performed numerically, however, it suffers from the round-off error because the function $\sin(x)/x$ decays quickly with increasing $|x|$. It has been found in the present problem that $K = 4$ yields convergence. When $t = t_i$, $\sin(x)/x$ is unity and the discrete signal is recovered as $x(t = t_i) = x_i$.

The interpolation equation (21) is a perfect filter for recovering a continuous signal from a discrete signal. The most spectacular property of this method is that both the mean and the root-mean-square (rms) of the continuous signal are identical to those of the discrete signal. In contrast, the spline and polynomial interpolations do not preserve the mean and the rms. Also, equation (21) is computationally short to evaluate and therefore is particularly suitable for applications such as the variable step size integration of equations of motion.

Testing

In summary, it is desirable to study the computational efficiency and the sensitivity of the required drift force signal to the following:

(*a*) changes in the location of the cutoff frequency,

(*b*) approximation of the original spectrum by a white spectrum,

(*c*) method used for generating the discrete signal at equal time intervals,

(*d*) changes in the duration of the time intervals,

(*e*) changes in the number of harmonics taken in the summations (10) and (11) of the IDFFT method and the cosine series method, respectively, and

(*f*) quality of interpolation using (21).

The testing procedure utilized was to assume an input spectrum approximating the original spectrum, then to generate the signal record, followed by a sampling of record and recomputation of the spectrum. The criteria used for evaluating the tests are

1. quality of the output spectrum (how well it preserves the original spectrum shape and area),
2. quality of the signal (smoothness, frequency, and magnitude of occurrences of local extrema, and how well it resembles the narrow-band signal), and
3. frequency content of the output spectrum (how wide can the frequency range be without making the signal too erratic).

The particulars of generating the output spectrum from the signal are given in Table 1; they are the same for all tests. The plots of the signal show only the first 1200 seconds (s) of the record, but the spectral computations are based on the entire record length of 15 000 s.

Table 2 lists the input and output particulars of the tests and Figs. 1 through 15 present the plotted results, one figure per test. The upper frame of each figure contains the input and output spectra. The input spectral heights are shown by circles and the output ones by a continuous line. The circles indicating the input spectra for the IDFFT method represent the initial spectrum which is linearly interpolated at the required number of frequencies to provide the spectrum input into the IDFFT. The lower frame of each figure contains the time records. The circles represent here the random signal, and the continuous line the signal interpolated by equation (21). The plots of the latter signal are generated from points interpolated at 5-s intervals. In all tests involving white spectra, the spectral heights have been adjusted to make the area under the spectrum equal to that of the corresponding original spectrum for the same range of frequencies. Three ranges of frequencies have been included in the tests (see Table 2). The largest cutoff frequency is equal to the Nyquist frequency of Table 1, that is, to the largest frequency that can be detected with the assumed record sampling interval. The two other ranges of frequency have been taken as a half and a quarter of the maximum range. The maximum resonant frequency occurs at 0.02 rad/s; thus all resonant

Table 2 Record simulation data

	Input Parameter						Output	
						Rms	Rms	
Test	Method	Spectrum Shape	ω_{max}, rad/s	No. of Harmonics[a]	Δ, s	Input Spectrum	Record	Output Spectrum
1	IDFFT	white	0.2	512	15	1.22	1.23	1.19
2	CS	white	0.2	30	15	1.22	1.21	1.22
3	IDFFT	original	0.2	512	15	1.22	1.24	1.24
4	CS	original	0.2	30	15	1.22	1.24	1.24
5	IDFFT	white	0.1	256	30	0.909	0.905	0.920
6	CS	white	0.1	30	30	0.909	0.903	0.909
7	IDFFT	original	0.1	256	30	0.909	0.944	0.951
8	CS	original	0.1	30	30	0.909	0.900	0.901
9	IDFFT	white	0.05	128	60	0.591	0.597	0.600
10	CS	white	0.05	30	60	0.591	0.593	0.590
11	IDFFT	original	0.05	128	60	0.591	0.598	0.596
12	CS	original	0.05	30	60	0.591	0.599	0.600
13	CS	original	0.2	70	15	1.22	1.23	1.26
14	CS	original	0.1	70	30	0.909	0.908	0.906
15	CS	original	0.05	70	60	0.591	0.592	0.592

[a] In one-sided spectrum for IDFFT method.

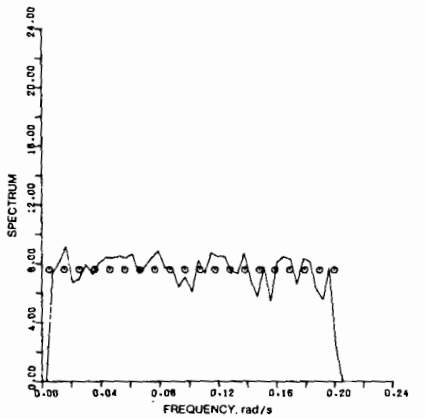

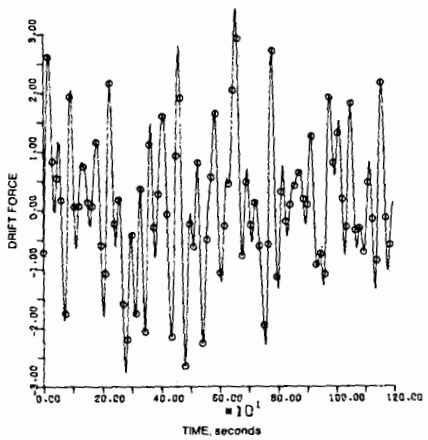

Fig. 1

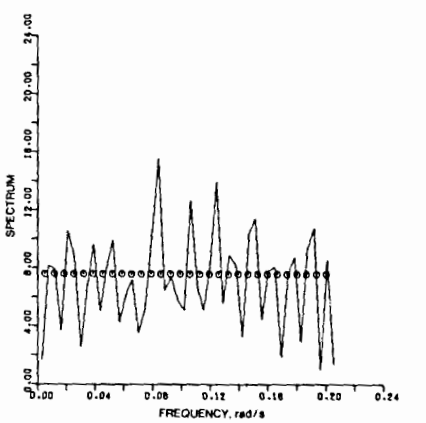

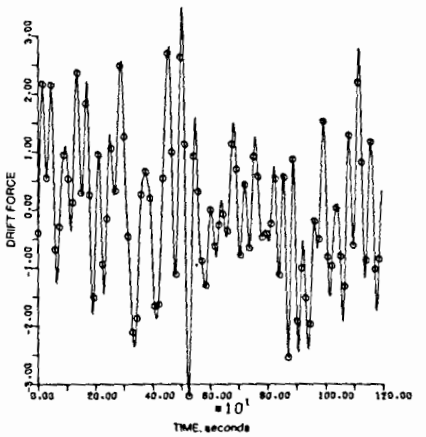

Fig. 2

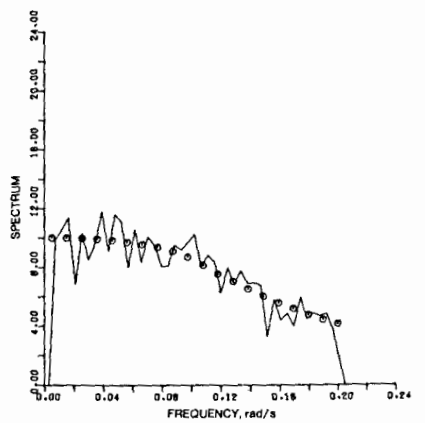

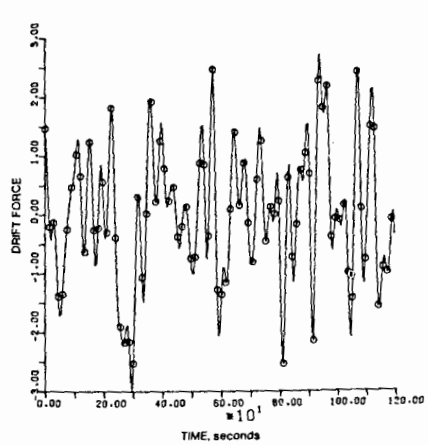

Fig. 3

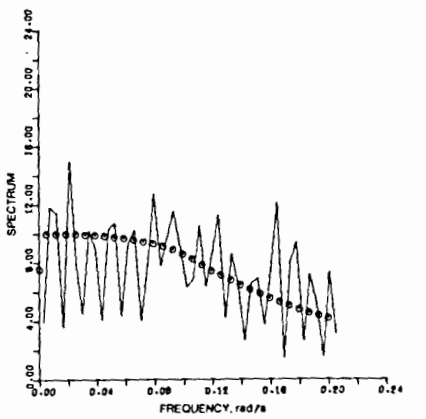

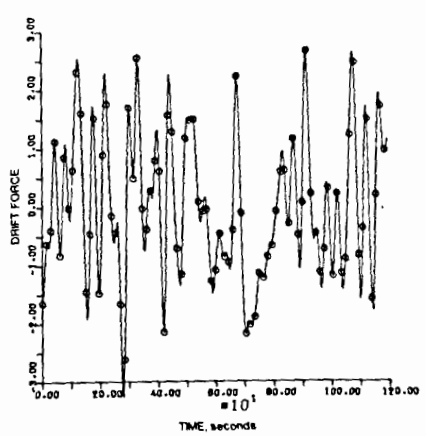

Fig. 4

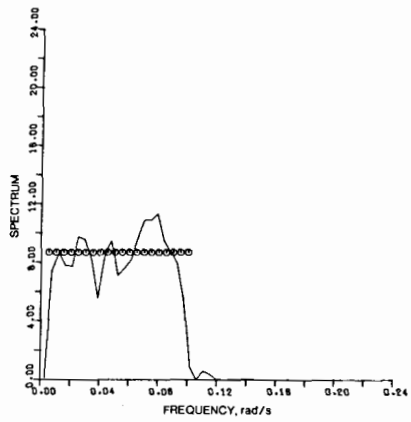

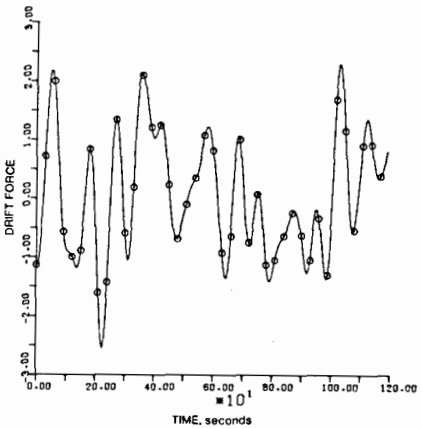

Fig. 5

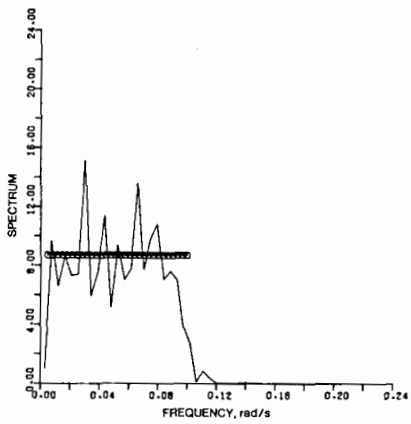

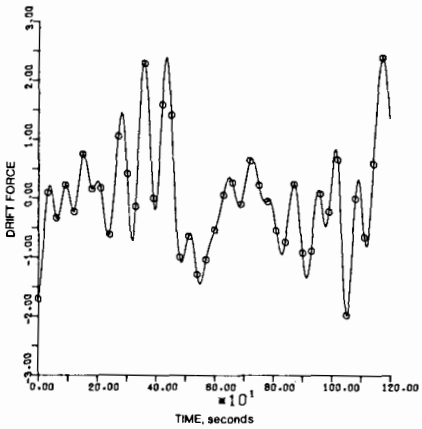

Fig. 6

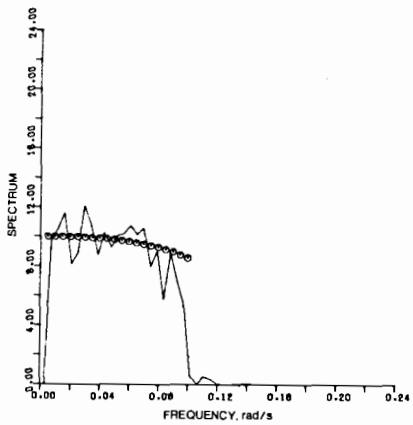

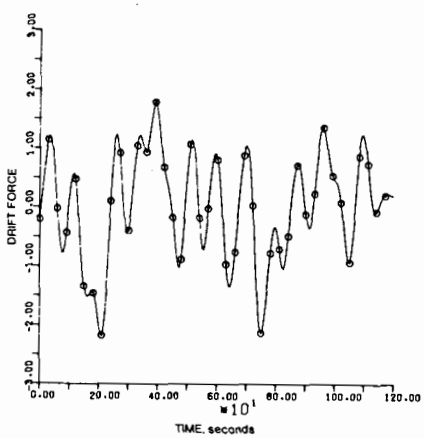

Fig. 7

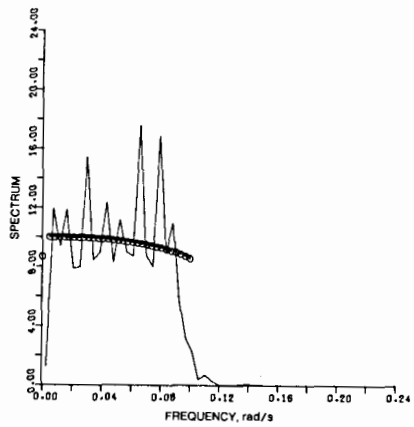

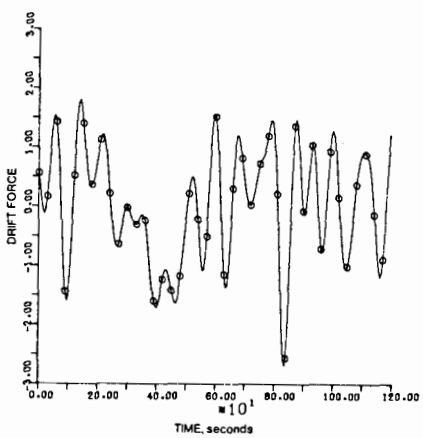

Fig. 8

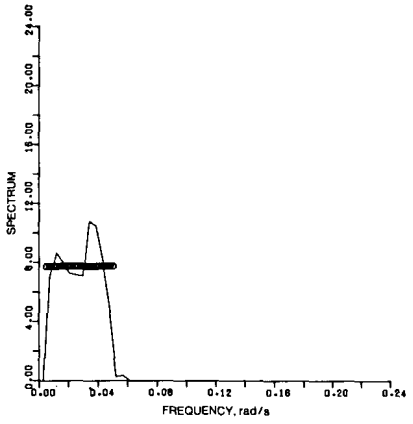

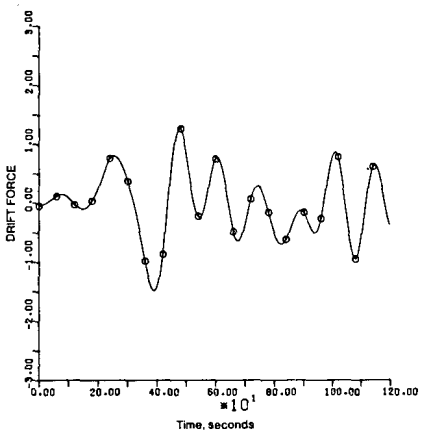

Fig. 9

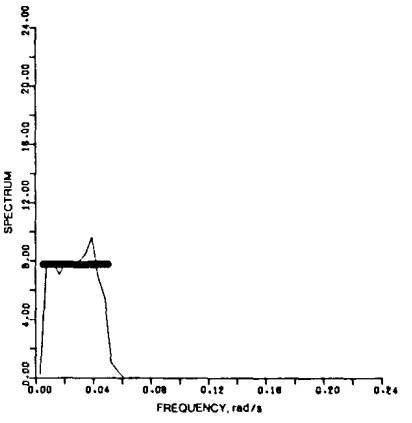

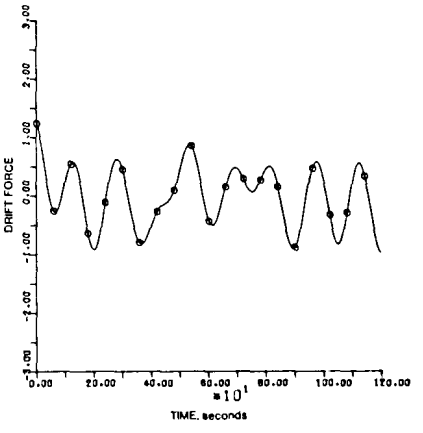

Fig. 10

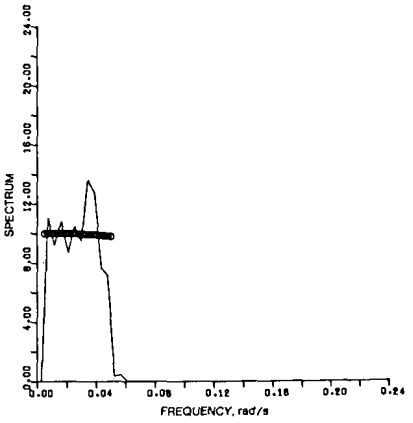

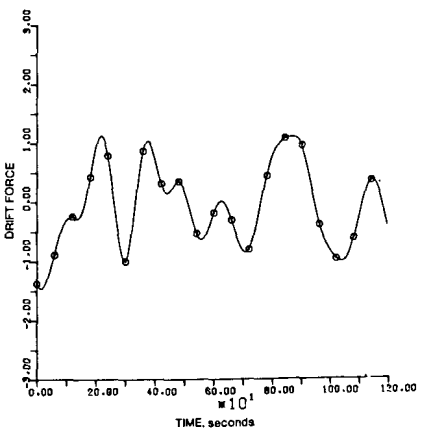

Fig. 11

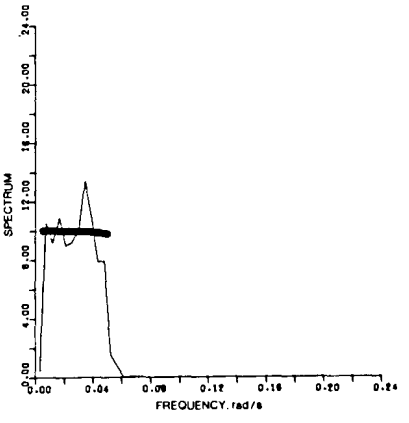

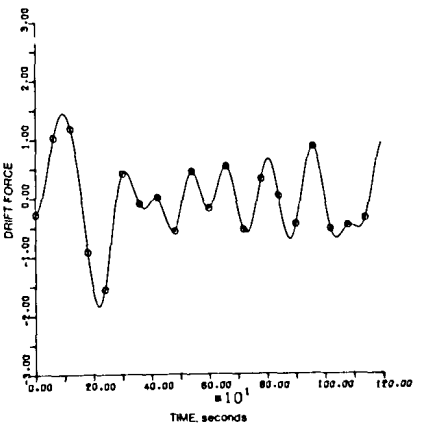

Fig. 12

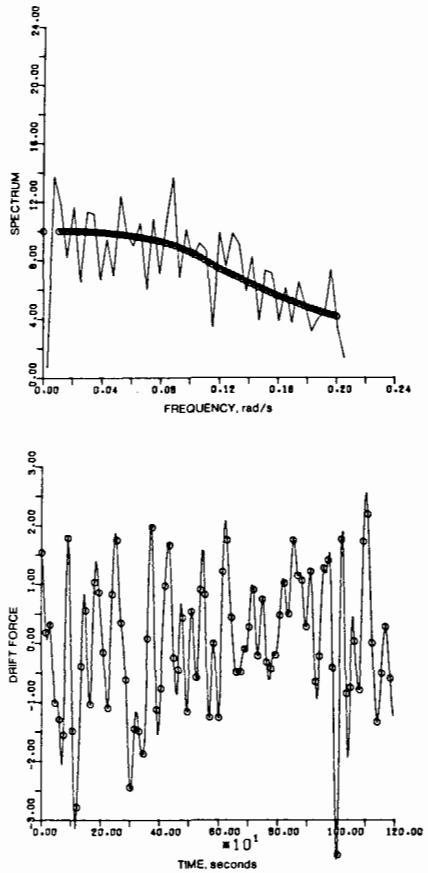

Fig. 13

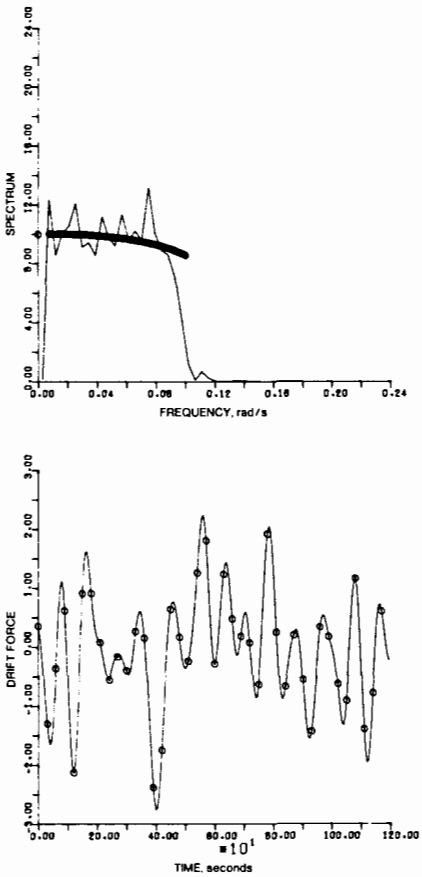

Fig. 14

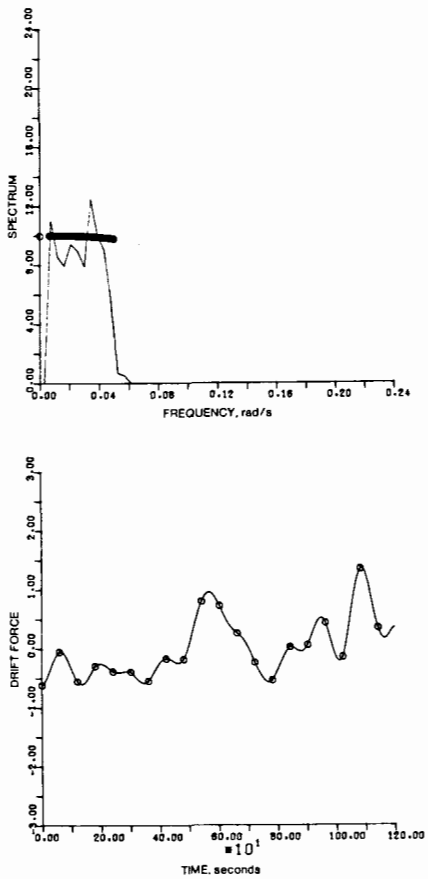

Fig. 15

frequencies are located well within the range of the drift excitation frequencies. The spectral heights for the full frequency range spectra have been adjusted so as to make the record signal nondimensional.

Results

The output parameters of Table 2 indicate that in all tests the agreement is satisfactory between the rms values computed from the input spectrum, from the interpolated record, and from the output spectrum. This is a reflection of the high quality of the $\sin(x)/x$-type interpolation.

A general comparison between the tests involving the IDFFT method and the cosine series method indicates that the IDFFT results in a much closer recovery of the spectral shapes. In fact, the IDFFT method would reproduce the spectral shape exactly, were it not for the cosine window applied to the interpolated records.

The computing time was consistently higher for the IDFFT method, by a factor of between 3 and 7.

Figures 1–4 represent the tests with the maximum range of frequencies. Figures 1 and 3 illustrate the white and original spectra for the IDFFT method and Figs. 2 and 4 similarly for the cosine series method. The character of all four records is almost identical. It could be expected that the white spectra would result in more occurrences of local extrema (peaks on the wrong side of the zero level) because of the larger relative contribution of the high-frequency harmonics. The tests do not indicate this, apparently because the differences between the white and "shaped" spectral heights are not large enough even at the high end of frequencies. The quality of the records is consistently poor in terms of their usefulness for the integration algorithm. The records are erratic, with large numbers of local extrema and with narrow peaks.

Figures 5–8 illustrate the tests with the intervals at which the random signals were generated, increased by a factor of 2 relative to the previous cases. Consequently the range of frequencies is now decreased by 2 also. Again, the records look almost identical to each other, but are much improved in comparison with those of Figs. 1–4. They are smoother and show more resemblance to a narrow-band signal. There are still relatively large numbers of local extrema.

Figures 9–12 demonstrate the tests with the interval halved again. As expected, the record smoothness is significantly improved and there are practically no local extrema. The range of frequencies is now so narrow that all frequencies are well within the flat portion of the original spectrum; therefore the approximations by the white spectrum are practically perfect.

All tests described in the preceding which involved the cosine series method were based on 30 harmonics used in equation (11). The corresponding tests with 70 harmonics are shown in Figures 13, 14, and 15 and these should be compared with Figures 4, 8, and 12, respectively. The spectral shapes are, not surprisingly, better reproduced with the larger number of harmonics. The records involving the interval lengths of 15 and 30 s (Figs. 13 and 14) look practically the same as before. Even with 70 terms, however, the spectrum shape is not as well preserved as was the case with the FFT method.

Conclusions

1. The interpolation using the $\sin(x)/x$ type is excellent.
2. The IDFFT method is not only more efficient computationally but it also reproduces the spectral shape better than does the cosine series method.
3. Both methods produce very similar records, other parameters being equal.
4. An increase in the number of harmonics used in the cosine series method slowly improves the quality of the spectral shape recovery, but it has little effect on the signal shape.
5. The approximation of the original spectrum shape by a white spectrum of equal area has practically no effect on the record behavior, even for a relatively large range of frequencies, and it can therefore be confidently used.
6. Increasing the spacing at which the random signal is generated improves significantly the smoothness and regularity of the record.
7. The tradeoff in the selection of the frequency range is strongly biased toward making the range small. The theoretical method by which equation (2) has been derived implies that μ is small. The smaller the range, the more justified is the very convenient approximation of the spectrum by a white spectrum. The typical resonance frequencies of moored vessels are also very small. The only argument which might be used in favor of an increased range of frequencies is that it may be desirable to have nonzero excitation at high frequencies in order to detect there the transfer functions of the system, or to detect the bifurcation nonlinear response, but, as demonstrated here, it would have to be done at the expense of signal quality.

In conclusion, the IDFFT method combined with the interpolation algorithm of type $\sin(x)/x$ appears to be an efficient and convenient tool for the simulation of the drift force excitation in the equations of motion.

Acknowledgment

The authors wish to thank Dr. J. K. Hammond of the Institute of Sound and Vibration, University of Southampton, for many discussions.

References

1 Pinkster, J. A., "Low-Frequency Phenomena Associated with Vessels Moored at Sea," Offshore Technology Conference Paper SPE-4837, Houston, Texas, 1974.

2 Shinozuka, M., "Digital Simulation of Random Processes in Engineering Mechanics with the aid of FFT Technique," *Proceedings*, Symposium on Stochastic Problems in Mechanics, University of Waterloo, Waterloo, Ontario, Canada, 1973.

3 Shinozuka, M., "Time and Space Domain Analysis in the Structural Reliability Assessment," *Proceedings*, Second International Conference on Structural Safety and Reliability, Technical University of Munich, Munich, Germany, 1977.

4 Newland, D. E., *An Introduction to Random Vibrations and Spectral Analysis*, Longman, London and New York, 1975.

5 Shinozuka, M., "Digital Simulation of Random Processes and Its Applications," *Journal of Sound and Vibration*, Vol. 25, No. 1, 1972.

6 Jenkins, G. M. and Watts, D. G., *Spectral Analysis and its Applications*, Holden-Day, 1968.